



Nature of active sites in Cu-LTA NH₃-SCR catalysts: A comparative study with Cu-SSZ-13

Taekyung Ryu¹, Hyojun Kim¹, Suk Bong Hong*

Center for Ordered Nanoporous Materials Synthesis, Division of Environmental Science and Engineering, POSTECH, Pohang 37673, Republic of Korea



ARTICLE INFO

Keywords:
NH₃-SCR
Cu-LTA
Cu-SSZ-13
Active sites
Fast SCR

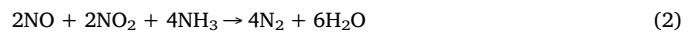
ABSTRACT

Here, a comparative study is made on four pairs of Cu-LTA and Cu-SSZ-13 zeolites with the same bulk Si/Al ratio (16) but different Cu/Al ratios (0.14–0.65), in an attempt to understand the similarities and differences in the nature of their catalytically active sites for the NH₃-SCR reaction. Two different types of copper ions, i.e., Cu²⁺ and [Cu(OH)]⁺, can exist in these two catalyst systems. However, their location and distribution were characterized to be quite different. Unlike the case in Cu-SSZ-13, both Cu²⁺ and [Cu(OH)]⁺ ions in Cu-LTA catalysts with Cu/Al ≤ 0.50 are predominantly located near the single 6-ring sites in the LTA structure, and copper species when over-exchanged reside within the 8-ring windows. It was also found that both Cu-SSZ-13 and Cu-LTA have nitrate and ammonium nitrate as reaction intermediates, but the relative amounts of these intermediates are always smaller in the latter catalyst system regardless of the Cu/Al ratio. This is primarily due to the preferential location of copper ions in single 6-rings that are spatially more confined than the 8-ring window sites. Consequently, Cu-LTA shows a better deNO_x activity under the fast SCR conditions than Cu-SSZ-13.

1. Introduction

There is an increased demand for fuel-efficient vehicles, leading to a wider use of lean burn diesel engines as a propulsion system for automobile applications. However, mitigating nitrogen oxides (NO_x) and soot productions from diesel engine combustion under highly oxidizing conditions remains as a challenging task to meet the ever-tightening global emission standards in automobile industries [1,2]. In fact, there is a general consensus that vehicle emission regulations will strengthen because of the new regulatory test procedures, such as WLTC and RDE, which reflect real vehicular operating conditions [3]. As a result, advanced diesel after-treatment systems consisting of multiple catalytic converters, i.e., diesel oxidation catalyst (DOC) and selective catalytic reduction (SCR) reactors, and diesel particulate filter, have received considerable attention as an essential part of the diesel powertrain system.

SCR of NO_x by NH₃ (NH₃-SCR) is one of the most promising technologies to eliminate NO_x from diesel engine exhaust under a wide operating temperature window [4–6]. Its three main reactions, depending on the NO₂/NO_x ratio, are as follows:



As the basic reaction of NH₃-SCR, reaction (1) is referred to as ‘standard’ SCR. By contrast, reaction (2), which include the use of equimolar amounts of NO and NO₂ (NO₂/NO_x = 0.5), proceeds at a much faster rate and is thus known as ‘fast’ SCR. To promote the latter SCR reaction, the DOC that oxidizes NO to NO₂ is commonly installed before the SCR converter in conventional diesel after-treatment systems [7,8]. However, in the presence of an excess amount (NO₂/NO_x > 0.5) of NO₂, NO_x reduction occurs at a slower rate than the other two reactions due to an inhibition phenomenon caused by the accumulation of ammonium nitrate on the SCR catalyst [9,10] and, hence, the reaction (3) is called ‘slow SCR’.

While copper-exchanged SSZ-13 (framework type CHA) has been successfully commercialized as an NH₃-SCR catalyst owing to its remarkable activity and durability compared to any of the earlier SCR catalysts [4,11], controlling the irreversible degradation of this zeolite-supported copper catalyst induced by the formation of copper oxides (CuO_x) that takes place upon hydrothermal treatment at 1073 K is still a major challenge [12]. Thus, considerable effort has been devoted not only to improving the hydrothermal stability of Cu-SSZ-13, but also to

* Corresponding author.

E-mail address: sbhong@postech.ac.kr (S.B. Hong).

¹ These authors contributed equally to this work.

finding other zeolite supports with better stability, suggesting, for example, zeolites SSZ-39 (AEI), SSZ-16 (AFX), and UZM-35 (MSE), as new catalyst supports [13–15]. However, none of these copper catalysts supported on zeolites have shown improved activity maintenance to meet the required level of deNO_x activity after hydrothermal aging at temperatures higher than 1073 K.

High-silica (Si/Al > 7.5) LTA zeolites, the synthesis procedures which have been recently reported by our group [16,17], serve as a remarkable support for copper catalysts with controllable metal loadings [16]. When divalent copper ions are fully exchanged into LTA zeolites with Si/Al ratios of 16 and 23, in particular, the resulting catalysts were found to show unrivaled activity maintenance even after hydrothermal aging at 1173 K, in stark contrast to the current commercial Cu-SSZ-13 catalyst [17,18]. The detailed characterizations reveal that the excellent hydrothermal stability of Cu-LTA catalysts is largely due to the location of divalent copper ions at the center of single 6-rings (*s*6rs) that act as a dealumination suppressor, as well as a catalytic center. We have also demonstrated that enhancement in low-temperature activity of Cu-LTA with Si/Al = 23 upon increasing hydrothermal aging temperatures up to 1173 K is attributed to the migration of Cu⁺ ions inside the *sod* cages to the vacant *s*6rs, together with their oxidation to Cu²⁺ ions [19].

This unprecedented hydrothermal stability of Cu-LTA catalysts has led us to investigate the intrinsic physicochemical properties of their active sites, which is essential in deciphering the molecular aspects of deNO_x catalysis. In fact, in search for new insights into the NH₃-SCR reaction over metal-exchanged zeolites, Cu-LTA has an advantage over Cu-SSZ-13, because of its remarkably symmetric support structure. Here we present the results obtained from DRIFT measurements of adsorbed NO and NH₃, temperature-programmed reduction of H₂, SCR kinetics, and *in situ* DRIFT measurements using NH₃, NO, and NO₂ molecules on four pairs of Cu-SSZ-13 and Cu-LTA catalysts with the same bulk Si/Al ratio (16) but different Cu/Al ratios (0.14–0.65) in an attempt to understand the similarities and differences in the nature of their active sites for the NH₃-SCR reaction. The overall characterization results allow us to explain why Cu-LTA has better performance under the fast SCR conditions than Cu-SSZ-13.

2. Experimental

2.1. Catalyst preparation

SSZ-13 and LTA zeolites with Si/Al = 16, which are ellipsoidal and cubic in shape with sizes of 1–1.5 and *ca.* 2 μm, respectively, were synthesized following the procedures in the literature [16,20]. As-made zeolites were calcined at 873 K in air for 8 h to eliminate the encapsulated organic structure-directing agents and converted into the ammonium form by stirring twice in 1.0 M NH₄NO₃ (2.0 g solid per 100 mL solution) at 353 K for 6 h. Four pairs of Cu-SSZ-13 and Cu-LTA catalysts with different Cu/Al ratios were prepared by stirring their ammonium form in 0.01 M Cu(CH₃COO)₂ (97%, Aldrich) aqueous solutions at room temperature. Here, the number and time of ion exchange were varied to achieve different levels of ion exchange, followed by drying at 363 K overnight and calcining at 823 K in air for 8 h. Here we refer to them as Cu-SSZ-13(I) – Cu-SSZ-13(IV) and Cu-LTA(I) – Cu-LTA(IV), respectively. The same Roman numerals in the catalyst identification indicate that each pair between the two catalyst systems has quite similar Cu/Al ratios or copper exchange levels (Table 1).

2.2. Characterization

Powder X-ray diffraction (XRD) patterns were recorded on a PANalytical X'Pert diffractometer (Cu Kα radiation) with an X'Celerator detector. Elemental analysis for Si, Al, and Cu was carried out by a combination of Shimadzu ICPE-9000 inductively coupled plasma and Perkin-Elmer 5000 atomic absorption spectrophotometer. N₂ BET

surface area measurements were carried out on a Mirae SI Nanoporosity-XG analyzer. X-ray absorption near edge structure (XANES) spectra at the Cu K-edge were collected at the 8C beamline of the PAL using a Si (111) crystal monochromator. Cu foil was used for energy calibration ($E_0 = 8979.0$ eV). The X-ray intensity was measured at room temperature before and after the sample with N₂-filled ionization chambers. Further details of the XANES measurements can be found elsewhere [18].

The IR spectra in the 4000–650 cm⁻¹ region were recorded on a Thermo-Nicolet 6700 FT-IR spectrometer equipped with an MCT detector and a DRIFT cell with ZnSe windows [21] and converted into Kubelka–Munk format using the Nicolet OMNIC software. Each spectrum was obtained by accumulating 64 scans at a spectral resolution of 4 cm⁻¹. Prior to IR measurements, a sample of 10 mg mounted in a ceramic holder was heated at 773 K under 21% O₂ in He flow for 60 min and cooled to the desired temperature. The total flow rate was kept at 100 mL min⁻¹ using mass flow controllers with a home-built cold-trap system. Background spectrum was collected in flowing He and subtracted from the sample spectrum for each measurement except those recorded in the OH region. Then, the difference DRIFT spectra of adsorbed NO or NH₃ were obtained after exposure of 500 ppm NO or 500 ppm NH₃ in He flow at room temperature for 60 min followed by purging with He for 30 min, respectively. For *in situ* DRIFT experiments, the difference DRIFT spectra were recorded as a function of exposure time during the stepwise introduction of reactant gases (e.g., first 500 ppm NO and 5% O₂ and then 500 ppm NH₃) balanced with He at 423 K, respectively. Spectral deconvolution was performed using the PeakFit curve-fitting program.

H₂ temperature-programmed reduction (TPR) was carried out on a Micromeritics AutoChem II 2920 analyzer. The sample was pretreated with 5% O₂ in Ar flow at 773 K for 60 min, cooled to room temperature, and then heated to 1073 K at a ramping rate of 10 K min⁻¹ with 5% H₂ in Ar flow. The TPR profiles obtained were deconvoluted using the PeakFit curve-fitting program. Temperature-programmed heating (TPH) measurements on the catalysts after the fast SCR reaction (NO₂/NO_x = 0.5) at 443 K were performed in the same reactor system described below. The catalysts were first exposed to a feed of 500 ppm NH₃, 250 ppm NO, 250 ppm NO₂, 5% O₂, 10% H₂O, and N₂ balance under 100,000 h⁻¹ GHSV at 443 K. After 60 min of exposure, NH₃, NO_x and O₂ were turned off. Then, the resulting catalysts were purged for 15 min in N₂ flow containing 10% H₂O. The TPH profile was recorded from 443 K to 873 K with a heating rate of 20 K min⁻¹.

2.3. Catalysis

The NH₃-SCR reaction was conducted under atmospheric pressure in a continuous fixed-bed flow reactor system [18,21]. Before each experiment, 0.6 g of catalyst pellets in the 20/30 mesh size packed into a 3/8-in.-od aluminum tube reactor were pretreated from room temperature to 773 K at a heating rate of 20 K min⁻¹ under 21% O₂ in N₂ flow (2000 mL min⁻¹) and kept at the desired reaction temperature for 2 h. The steady-state NO_x conversion was measured over the temperature range 433–873 K at a gas hourly space velocity (GHSV) of 100,000 h⁻¹. A feed gas stream containing 500 ppm NH₃, 500 ppm NO, 5% O₂, 10% H₂O, and N₂ balance was supplied through mass flow controllers. If required, 500 ppm NO_x (NO + NO₂) instead of 500 ppm NO was injected into the feed in order to vary the NO₂/NO_x ratio from 0 to 1. The NO oxidation was performed under the identical standard feed gas reaction conditions mentioned above, except that the NH₃ feed was excluded, and the catalytic results obtained were calibrated by subtracting the background NO₂ formation. The concentrations of the inlet and outlet gas composition were determined online by a Thermo-Nicolet 6700 FT-IR spectrometer equipped with a 2-m gas cell.

The turnover frequency (TOF) values for NH₃-SCR were calculated by the following equation:

Table 1

Chemical compositions of four pairs of Cu-SSZ-13 and Cu-LTA zeolite catalysts with different Cu/Al ratios and their catalytic properties for standard NH₃-SCR.

Catalyst ID	Cu ^a (wt %)	Si/Al ^a	Cu/Al ^a	Copper ion exchange level ^a (%)	<i>E</i> _{app} (kJ mol ⁻¹) ^b	lnA ^c	TOF × 10 ³ (s ⁻¹) ^d
Cu-SSZ-13(I)	0.88	16	0.15	30	67	12	2.2
Cu-SSZ-13(II)	2.00	16	0.34	68	72	13	1.5
Cu-SSZ-13(III)	2.78	16	0.49	98	73	13	0.9
Cu-SSZ-13(IV)	3.50	16	0.63	126	74	14	0.6
Cu-LTA(I)	0.85	16	0.14	28	40	4	0.5
Cu-LTA(II)	1.90	16	0.32	64	43	4	0.7
Cu-LTA(III)	2.70	16	0.48	96	44	5	0.9
Cu-LTA(IV)	3.30	16	0.65	130	62	9	0.4

^a Determined by elemental analysis.

^b Calculated from the Arrhenius plots for the standard SCR reaction in Fig. 4.

^c The natural logarithm of the pre-exponential factor for the effective collision between the intrazeolitic copper species and the reactant molecules.

^d Determined at 443 K.

$$TOF (s^{-1}) = \frac{C_{NO} \times X_{NO} \times \nu}{\left(\frac{ML}{MW}\right)} \quad (4)$$

where C_{NO} , X_{NO} , and ν are NO concentration (mol mL⁻¹), NO conversion (%), volumetric flow rate (mL s⁻¹), respectively. Also, ML and MW are the copper loading (g) on the catalyst and the molecular weight (63.54 g mol⁻¹) of copper, respectively. The apparent activation energy (E_{app}) and pre-exponential factor (lnA) were calculated from the slope and intercept of the Arrhenius plot, respectively. The steady-state NO_x conversion over the differential reactor containing 0.15 g of the catalyst in the 20/30 mesh was maintained below 20% under standard feed gas composition at the reaction temperatures below 473 K under 500,000 h⁻¹ GHSV in order to keep the reaction in the kinetic regime.

3. Results and discussion

3.1. General characterization

The chemical compositions of a series of Cu-SSZ-13 and Cu-LTA catalysts prepared here are listed in Table 1. Since they possess precisely controlled compositions, comparison of their characterization and catalytic data will allow us to understand the characteristics of active sites in Cu-LTA for NH₃-SCR. The powder XRD patterns of these catalysts with different zeolite support structures and/or Cu/Al ratios are in excellent agreement with those of zeolite supports (i.e., H-SSZ-13 or H-LTA), except for minor differences in the relative X-ray peak intensity (Supplementary Fig. S1). This indicates that they maintain structural integrity during the copper ion exchange followed by calcining at 823 K, as further confirmed by the N₂ BET surface area data in

Supplementary Fig. S1. A small decrease in the N₂ BET surface area of the Cu-SSZ-13 and Cu-LTA catalysts with higher Cu/Al ratios may in our view be attributed to an increase in amount of intrazeolitic copper species, e.g., Cu²⁺ and/or [Cu(OH)]⁺.

Cu K-edge XANES spectroscopy shows that the copper species in each catalyst are present mainly as the divalent cation: copper oxide (CuO_x) species are hardly detectable (Supplementary Fig. S2) [18,21]. However, it is well known that the Cu²⁺ ions in copper-exchanged zeolites can also exist in the form of [Cu(OH)]⁺ ions [22–25]. As shown in Supplementary Fig. S3, in fact, we were able to observe an OH IR band around 3655 and 3670 cm⁻¹, assignable to the [Cu(OH)]⁺ ions in Cu-SSZ-13 and Cu-LTA catalysts, respectively, the intensity of which becomes gradually stronger with increasing Cu/Al ratio [24,25]. Despite their high Cu/Al ratios (ca. 0.5 or higher; ≥ 100% exchange levels), in addition, the IR spectra of Cu-LTA(III) and Cu-LTA(IV) still exhibit two OH bands around 3620 and 3550 cm⁻¹ corresponding to the bridging Si–OH-Al groups (Brønsted acid sites) pointed into the *lta* cages and positioned at the *s6r* centers of *sod* cages, respectively [18]. If all copper species in these catalysts are present exclusively as Cu²⁺ ions, there should then be no detectable bridging OH bands. Therefore, some Cu²⁺ ions in Cu-LTA(III) and Cu-LTA(IV) appear to exist as [Cu(OH)]⁺, like in Cu-SSZ-13.

3.2. Nature of active sites

To investigate the local environment of Cu²⁺ species in Cu-LTA, we measured the difference DRIFT spectra of adsorbed NO on four pairs of Cu-SSZ-13 and Cu-LTA catalysts with the same bulk Si/Al ratio (16) but different Cu/Al ratios (0.14–0.65). Fig. 1 compares their spectra in the

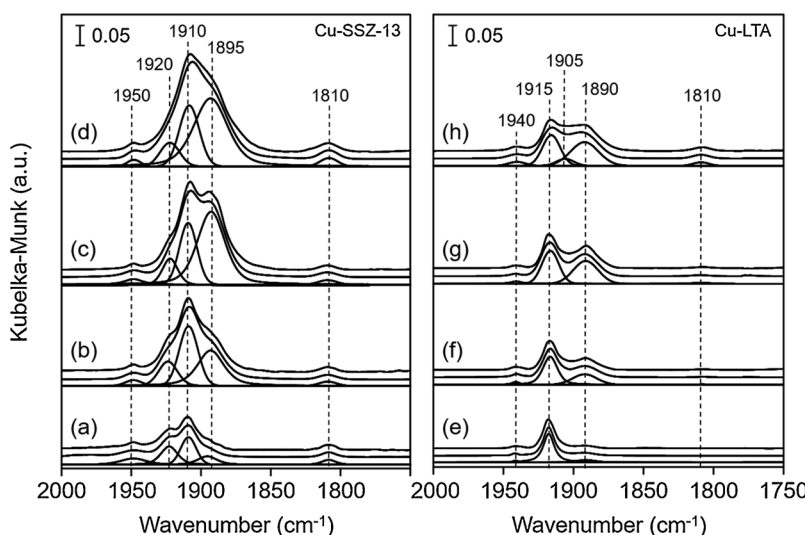


Fig. 1. Difference DRIFT spectra of adsorbed NO on (a) Cu-SSZ-13(I), (b) Cu-SSZ-13(II), (c) Cu-SSZ-13(III), (d) Cu-SSZ-13(IV), (e) Cu-LTA(I), (f) Cu-LTA(II), (g) Cu-LTA(III), and (h) Cu-LTA(IV) catalysts: experimental (top); simulated (middle); deconvoluted components (bottom). All the spectra were collected at 298 K after exposure to 500 ppm NO in He flow for 60 min followed by purging with He for 30 min. Prior to NO adsorption, each catalyst was oxidized at 773 K for 120 min.

2000–1750 cm⁻¹ region for the NO molecules adsorbed on intrazeolitic Cu²⁺ and Cu⁺ ions [23,26]. In addition to two weak band around 1950 and 1810 cm⁻¹ assignable to the NO species on the Cu²⁺ ions at double 6-rings (*d*6rs) and the Cu²⁺ auto-reduction during catalyst activation, deconvolution of the difference DRIFT spectra of Cu-SSZ-13 catalysts shows signs of three components around 1920, 1910, and 1895 cm⁻¹ which can be assigned to adsorbed NO species on the [Cu(OH)]⁺ ions within the 8-ring windows of *cha* cages [21,27]. There are no noticeable changes in the intensity of the band around 1950 cm⁻¹ as the Cu/Al ratio increases from 0.15 to 0.63 (Table 1), which is also the case of one deconvoluted component around 1920 cm⁻¹. However, the other two components, especially the one around 1895 cm⁻¹, gives a clear increase in intensity. As previously reported [21], therefore, the concentration of [Cu(OH)]⁺ ions within the 8-ring windows of Cu-SSZ-13 increases with increasing the Cu/Al ratio, unlike that of Cu²⁺ ions on *d*6rs.

Spectral deconvolution also shows that the number and relative intensity of deconvoluted components differ notably according to the framework type of zeolite supports, as well as to the Cu/Al ratio of zeolite-supported copper catalysts. For example, the DRIFT spectrum of Cu-LTA(III) with Cu/Al = 0.48 displays a weak band around 1940 cm⁻¹. It should be noted that this spectrum exhibits only two bands around 1920 and 1890 cm⁻¹, unlike that of Cu-SSZ-13(III) with a quite similar Cu/Al ratio (0.49) characterized by three bands in the same region (Fig. 1), indicating the existence of differences in the location and distribution of copper ions between the two catalyst systems. Prior to our work, no studies have been attempted to elucidate the interactions between NO and copper ions in LTA-type zeolites using IR spectroscopy, mainly due to the poor thermal stability of zeolite supports. However, there is a DRIFT study on adsorbed NO on the nearly fully copper-exchanged zeolite Y (FAU) with Si/Al = 2.7, where three bands at 1955, 1923, and 1880 cm⁻¹ were observed [26]. The former two bands are assigned to the NO molecules adsorbed on the Cu²⁺ ions positioned adjacent to the *s*6r centers connecting the *sod* cages with the *Y* supercages, although the latter one has yet to be elucidated.

It is worth noting that the location of Cu²⁺ ions in Cu-Y is similar to that of a fully copper-exchanged LTA, i.e., Cu-LTA(III), where the Cu²⁺ ions exclusively exist at the *s*6r centers connecting the *sod* cages and the larger *lta* cages [18]. This led us to assign the two bands appearing around 1940 and 1920 cm⁻¹ in the DRIFT spectra of Cu-LTA catalysts to the NO species adsorbed on the Cu²⁺ ions at *s*6r centers, because their positions are similar to those of the bands observed for Cu-Y [26]. As already discussed above (Supplementary Fig. S3), on the other hand, the copper ions in Cu-LTA catalysts, especially in Cu-LTA(III) and Cu-LTA(IV), can exist as [Cu(OH)]⁺, as well as Cu²⁺. Since the NO molecules are more strongly adsorbed on [Cu(OH)]⁺ than on Cu²⁺, giving a lower frequency for the NO stretching vibration [28], the band around 1890 cm⁻¹ in the spectra of Cu-LTA catalysts can be assigned to adsorbed NO on the [Cu(OH)]⁺ ions at *s*6r centers. Although experimentally unobserved yet, in fact, theoretical calculations on Cu-SSZ-13 have suggested that [Cu(OH)]⁺ ions can be located not only within 8-ring windows, but also on *d*6r [28]. Fig. 1 also shows that besides the three bands around 1940, 1920, and 1890 cm⁻¹, the relative intensities of which are similar to those of the corresponding bands in the spectrum of Cu-LTA(III), the DRIFT spectrum of Cu-LTA(IV) with the highest Cu/Al ratio (0.65) exhibits a new band around 1905 cm⁻¹, suggesting the presence of another site for over-exchanged copper species, probably within 8-ring windows (see below).

Fig. 2 shows the difference DRIFT spectra in the zeolite framework region of four Cu-SSZ-13 and four Cu-LTA catalysts with different Cu/Al ratios recorded at room temperature after exposure to 500 ppm NH₃ in He flow. The Cu-O bond formation in copper-exchanged zeolites can perturb the T-O-T vibrations of the zeolite support framework, thus being useful in the identification of different types of intrazeolitic Cu sites [29–32]. In particular, it has been recently reported that the copper ions in zeolites saturated with NH₃ interact more strongly with

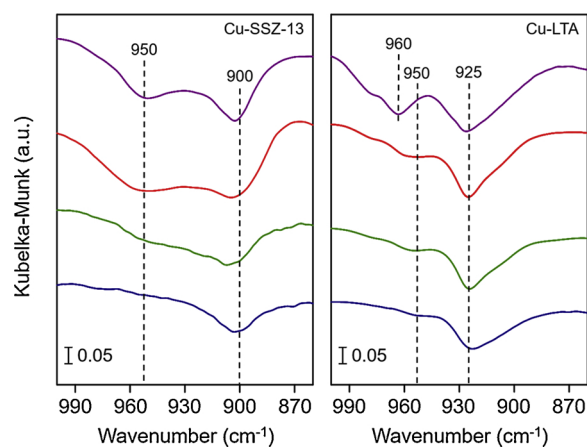


Fig. 2. Difference DRIFT spectra in the structural region of (left, from bottom to top) Cu-SSZ-13(I), Cu-SSZ-13(II), Cu-SSZ-13(III), and Cu-SSZ-13(IV) catalysts and (right, from bottom to top) Cu-LTA(I), Cu-LTA(II), Cu-LTA(III), and Cu-LTA(IV) catalysts recorded at 298 K after exposure to 500 ppm NH₃ in He flow for 60 min followed by purging with He for 30 min. Prior to NH₃ adsorption, each catalyst was oxidized at 773 K for 120 min.

the negatively charged framework oxygen atoms, yielding better-resolved, negatively perturbed T-O-T vibration bands [32]. As shown in Fig. 2, a negative band around 900 cm⁻¹ is observable in the difference DRIFT spectra of all four Cu-SSZ-13 catalysts. With increasing Cu/Al ratio from 0.15 to 0.63, in addition, a new band around 950 cm⁻¹ becomes more visible, which is in line with the study by Luo et al [32]. These two perturbed T-O-T bands around 900 and 950 cm⁻¹ have been attributed to the Cu²⁺ ions on *d*6rs and the [Cu(OH)]⁺ ions within the 8-ring windows in Cu-SSZ-13, respectively.

While the difference DRIFT spectrum of Cu-LTA(I) with the lowest Cu/Al ratio (0.14) is essentially the same as that of its counterpart, i.e., Cu-SSZ-13(I), except the difference in the position (*ca.* 925 vs 900 cm⁻¹) of a strong negative band, it exhibits a weaker but non-negligible band around 950 cm⁻¹. As shown in Fig. 2, in addition, an increase in intensity of the band around 950 cm⁻¹ with increasing Cu/Al ratio to 0.48 (nearly 100% Cu²⁺ exchange) is significantly lower than that of the corresponding band in the spectra of Cu-SSZ-13 catalysts. More interestingly, the spectrum of over-exchanged Cu-LTA(IV) with Cu/Al = 0.65 displays a new strong negative band around 960 cm⁻¹, indicating the existence of another Cu site, which is not present in the other three Cu-LTA catalysts with lower Cu/Al ratios. When combined with the DRIFT results in Fig. 1, therefore, the two negative bands around 925 and 950 cm⁻¹ can be assigned to the T-O-T perturbation of the LTA framework by the Cu²⁺ and [Cu(OH)]⁺ ions balanced with two and one negative framework charges in *s*6rs, respectively. In addition, it is most likely that the band around 960 cm⁻¹ may originate from the perturbation by the copper ions located within the 8-ring windows of *lta* cages in Cu-LTA(IV), mostly by the [Cu(OH)]⁺ ions. This is because the hydrothermal stability of Cu-LTA(IV), where the excess copper ions must reside within its 8-ring windows, is considerably poorer than the other three Cu-LTA catalysts with lower Cu/Al ratios [18].

Fig. 3 shows the H₂ TPR profiles of four pairs of Cu-SSZ-13 and Cu-LTA catalysts with different Cu/Al ratios. The reduction peak with a maximum in the temperature region 470–670 K can be due to the reduction of Cu²⁺ to Cu⁺ [30,33]. No significant differences in the area of this peak in the TPR profiles of each pair are observed. As shown in Fig. 3, however, the area and position of the higher-temperature reduction peak corresponding to the reduction of Cu⁺ to Cu° is more dependent on the Cu/Al ratio. For example, while the profile of Cu-SSZ-13(I) gives no peak in the temperature region higher than 800 K, the reduction of Cu⁺ to Cu° in Cu-SSZ-13 becomes more apparent in the lower temperature region with an increasing Cu/Al ratio to 0.63. This

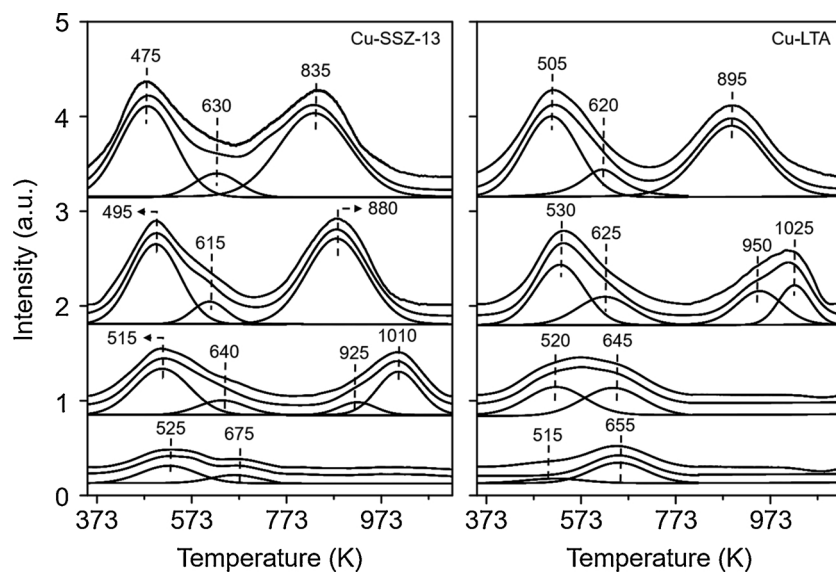


Fig. 3. H₂ TPR profiles of (left, from bottom to top) Cu-SSZ-13(I), Cu-SSZ-13(II), Cu-SSZ-13(III), and Cu-SSZ-13(IV) catalysts and (right, from bottom to top) Cu-LTA(I), Cu-LTA(II), Cu-LTA(III), and Cu-LTA(IV) catalysts: experimental (top); simulated (middle); deconvoluted components (bottom).

clearly shows that the reduction of Cu⁺ to Cu° in Cu-SSZ-13 is easier at a higher Cu/Al ratio, probably due to an increase in concentration of [Cu(OH)]⁺ ions that may make the monovalent copper species less stable. A quite similar result has long been observed for a series of Cu-ZSM-5 (MFI) catalysts with the same Si/Al ratio (14) but different Cu/Al ratios (0.19–0.59) [33].

On the other hand, the lack of a high-temperature (> 800 K) reduction peak in the H₂ profile of Cu-LTA(II), which is completely different to Cu-SSZ-13(II), suggests that the interactions of copper ions with the zeolite frameworks are stronger in Cu-LTA than in Cu-SSZ-13. This can be further supported by the fact that the positions of the high-temperature reduction peak in the profiles of Cu-LTA(III) and Cu-LTA(IV) are at higher temperatures than those observed for Cu-SSZ-13(III) and Cu-SSZ-13(IV), respectively. Fig. 3 also shows that like the case of Cu-SSZ-13 catalysts [30], the low-temperature (470–670 K) reduction peak corresponding to the reduction of Cu²⁺ to Cu⁺ in the H₂ TPR profiles of all four Cu-LTA catalysts can be deconvoluted into two components with maxima in the temperature ranges 500–520 and 640–660 K. It is interesting to note that the area of the first low-temperature reduction peak is almost independent of the Cu/Al ratio of Cu-LTA catalysts, whereas the opposite is true for the second low-temperature reduction peak. When correlated with the DRIFT results in Figs. 1 and 2, therefore, we assign these two low-temperature reduction peaks to the reduction of [Cu(OH)]⁺ and Cu²⁺ ions at s6rs in Cu-LTA, respectively.

Fig. 4 shows the Arrhenius plots of the four pairs of Cu-SSZ-13 and

Cu-LTA catalysts with different Cu/Al ratios for the standard SCR reaction in the low-temperature region (< 473 K). The apparent activation energy (E_{app}) and pre-exponential factor (lnA) for the corresponding catalysts calculated from these plots are listed in Table 1. The E_{app} and lnA values (67–74 kJ mol⁻¹ and 12–14, respectively) for Cu-SSZ-13 catalysts correspond well with those in the literature [34,35], confirming that the nature of their active sites remains unaltered by the Cu/Al ratio. However, the turnover frequency (TOF) for reduction of NO molecules per mole of copper ions gradually decreases with increasing Cu/Al ratio in the temperature range studied. This can be explained by intracrystalline diffusion limitation owing to the small size (3.8 × 3.8 Å) of 8-ring windows in Cu-SSZ-13 catalysts [36,37]. As corroborated by the DRIFT and H₂ TPR results in Figs. 1–3, the copper ions, mainly [Cu(OH)]⁺ ions, become more prevalent within 8-ring windows than on d6rs with an increase in its content. If such is the case, those species when coordinated with NH₃ and/or H₂O molecules may effectively hinder pore diffusion, resulting in the inefficient utilization as catalytically active sites for NH₃-SCR.

The catalytic results in Table 1 also show no noticeable differences (40–44 kJ mol⁻¹ and 4–5, respectively) in the E_{app} and lnA values for the three Cu-LTA catalysts with Cu/Al ≤ 0.48. Their E_{app} values are marginally higher than the value (38 kJ mol⁻¹) of an Cu-LTA catalyst with Si/Al = 23 and Cu/Al = 0.50 [19], where only s6rs serve as active Cu sites, but they are fairly smaller than those of the Cu-SSZ-13 counterparts. In contrast to that of Cu-SSZ-13, in addition, the TOF value of Cu-LTA gradually increases as the Cu/Al ratio approaches 0.50 (100%

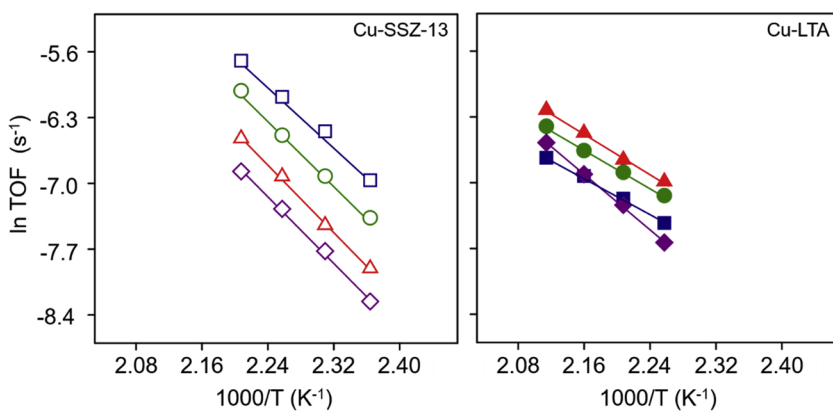


Fig. 4. Arrhenius plots for standard SCR over Cu-SSZ-13(I) (□), Cu-SSZ-13(II) (○), Cu-SSZ-13(III) (△), Cu-SSZ-13(IV) (◇), Cu-LTA(I) (■), Cu-LTA(II) (●), Cu-LTA(III) (▲), and Cu-LTA(IV) (◆). The feed contains 500 ppm NH₃, 500 ppm NO, 5% O₂, 10% H₂O balanced with N₂ at 500,000 h⁻¹ GHSV. SCR kinetic data were obtained while maintaining NO_x conversion below 20% within the differential regime.

exchange level; Fig. 4). This suggests that the intracrystalline diffusion effects on the NH₃-SCR activity of Cu-LTA when Cu/Al ≤ 0.50 may be negligible, probably owing to the absence of copper species in within the 8-ring windows. However, the fact that Cu-LTA(IV) was calculated to have a considerably higher E_{app} value (62 kJ mol⁻¹; Table 1) strongly suggests that the main active sites of this over-exchanged Cu-LTA catalyst is intrinsically different from those of Cu-LTA catalysts with Cu/Al ≤ 0.50. In particular, its pre-exponential factor (9) signifies the high probability of collision between the reactants and Cu active sites. Therefore, we again conclude that the over-exchanged copper species in Cu-LTA(IV) are mainly located within the 8-ring windows, as recently proposed for Cu-SSZ-13 [38].

3.3. Reaction intermediates

To more thoroughly understand the differences in the catalytic properties of Cu-SSZ-13 and Cu-LTA catalysts for NH₃-SCR, we investigated the formation of reaction intermediates over these catalysts using *in situ* DRIFT spectroscopy during exposure to a mixture of NO and O₂ at 423 K. As shown in Supplementary Fig. S4, when the Cu-SSZ-13 catalysts are exposed to a mixture of NO and O₂ for up to 30 min, there is a continuous increase in intensity of a broad band in the 1650–1550 cm⁻¹ region, which is subsequently resolved into three bands around 1625, 1610, and 1570 cm⁻¹ due to the nitrate (NO₃⁻) ions generated on Cu sites [39] with increasing exposure time to 30 min. This trend is more apparent as the Cu/Al ratio increases from 0.15 to 0.63. A similar trend can be observed in the DRIFT spectra of Cu-LTA catalysts. We should note here that while NO₃⁻ is known as one of the key reaction intermediates for the NH₃-SCR reaction over metal-exchanged zeolite catalysts [5,40,41], the two bands around 1610 and 1570 cm⁻¹ corresponding to bidentate NO₃⁻ are fairly poorly resolved in the spectra of Cu-LTA catalysts compared to their Cu-SSZ-13 counterparts. This again shows notable differences in the local environments of copper ions between Cu-LTA and Cu-SSZ-13. Given that bidentate NO₃⁻ is primarily formed on the [Cu(OH)]⁺ ions in Cu-SSZ-13 [42,43], comparison of the relative intensities of their bands, i.e., of those appearing around 1610 and 1570 cm⁻¹, reveals that the concentration of [Cu(OH)]⁺ ions in Cu-LTA is only 20% or smaller of that observed for Cu-SSZ-13, especially when the Cu/Al ratio is lower than 0.50 (Supplementary Fig. S4).

No noticeable changes in the DRIFT spectra of Cu-SSZ-13 and Cu-LTA catalysts were caused by He purging at 423 K after NO₃⁻ formation. As shown in Fig. 5, however, their NO₃⁻ bands in the 1650–1550 cm⁻¹ region become diminished upon exposure to NH₃. Simultaneously, two new broad bands appear around 1620 and 1460 cm⁻¹, which are attributed to the adsorption of NH₃ onto Lewis (copper ions) and Brønsted (zeolite protons) acid sites, respectively [44]. This clearly shows that the NO₃⁻ species generated in Cu-SSZ-13 and Cu-LTA catalysts are reduced by NH₃ [45]. A more important observation from Fig. 5 is that the rate of NO₃⁻ disappearance is much faster in Cu-LTA than in Cu-SSZ-13, regardless of the Cu/Al ratio, probably due to the considerably smaller concentration of this anion in the former catalyst rather than to its higher reactivity with NH₃. This can be further supported by the fairly low NO oxidation activity of Cu-LTA catalysts compared to Cu-SSZ-13 catalysts (Supplementary Fig. S5), because NO has to be oxidized first to NO₂ in order to form NO₃⁻ over copper-exchanged zeolite catalysts [41,45]. Therefore, it is most likely that the formation of NO₃⁻ species, which may play a significant role in initiating the NH₃-SCR reaction, does not proceed effectively over the Cu²⁺ ions at *s6rs* in Cu-LTA, explaining its lower standard SCR activity at low temperatures (< 523 K) than Cu-SSZ-13 (see below).

The argument given above can be further supported by another series of *in situ* DRIFT measurements using NO₂ at 423 K (Supplementary Fig. S6): the spectra of both series of Cu-SSZ-13 and Cu-LTA catalysts pre-saturated by NH₃ show two broad bands around 1620 and 1460 cm⁻¹ assignable to the adsorption of NH₃ onto Lewis

and Brønsted acid sites, respectively. However, the subsequent exposure to NO₂ for 30 min resulted in the disappearance of the former band around 1620 cm⁻¹, together with the appearance of two broad IR bands around 1600 and 1575 cm⁻¹ assigned to ammonium nitrate (NH₄NO₃) [45], an important intermediate which can be formed by the reaction between NO₂ and NH₃ when NO₂/NO_x ratio is 0.5 or higher [40]. Whereas these two bands become stronger in intensity with increasing Cu/Al ratio, there are no significant changes in the intensity of the band around 1460 cm⁻¹ corresponding to the adsorbed NH₃ on Brønsted acid sites during the exposure of NO₂. This suggests that the formation of NH₄NO₃ mainly occurs over the Lewis (copper ions) acid sites in both catalyst systems.

Like the case of NO₃⁻, the NH₄NO₃ intermediate generated in the four pairs of Cu-SSZ-13 and Cu-LTA catalysts is stable during He purging at 423 K. As shown in Fig. 6, however, the two broad bands around 1600 and 1575 cm⁻¹ gradually decrease upon exposure to NO, with the exception of Cu-SSZ-13(I) and Cu-LTA(I) with the lowest Cu/Al ratio among the catalysts employed. This implies the existence of a threshold Cu/Al ratio (or a concentration of copper ions) in catalysts investigated here for the reduction of NH₄NO₃ by NO. Since NH₄NO₃ is stable at temperatures below 473 K [9], it can be easily deposited on the zeolite pores, rendering the reactant molecules less accessible to catalytically active sites [45]. While the two bands around 1600 and 1575 cm⁻¹ corresponding to NH₄NO₃ are heavily overlapped with those from bidentate NO₃⁻, on the other hand, this is not the case of a relatively narrower band appearing around 1625 cm⁻¹ assigned to bridging NO₃⁻. Thus, this band can be used as an indicator of NO₃⁻ formation in Cu-SSZ-13 and Cu-LTA by NH₄NO₃ reduction in the presence of NO [45].

Fig. 6 also shows that the DRIFT spectra of all catalysts except Cu-SSZ-13(I) and Cu-LTA(I) are characterized by the evolution of a new band around 1625 cm⁻¹ with increasing NO exposure time at 423 K. The evolution rate of this band is considerably saturated when exposed to NO for 15–25 min. Of particular interest is that two broad bands appearing around 1600 and 1575 cm⁻¹, which are both attributable to NH₄NO₃, are hardly detectable or weak in the spectra of Cu-LTA catalysts with 0.32–0.65. However, these bands are still clearly observable in the spectra of the corresponding Cu-SSZ-13 catalysts with different Cu/Al ratios. Therefore, it is clear that even after 30 min of NO exposure, the three Cu-SSZ-13 catalysts with Cu/Al ratios higher than 0.15 have a non-negligible amount of NH₄NO₃, unlike the case of the corresponding Cu-LTA catalysts.

Fig. 7 compares the relative amounts of NO₃⁻ and NH₄NO₃ intermediates formed in Cu-SSZ-13 and Cu-LTA as a function of the catalyst Cu/Al ratio, which were determined from their DRIFT spectra (bottom traces of each panel in Figs. 5 and 6, respectively) measured at 423 K after exposure to 500 ppm NO and 5% O₂ in He flow and 500 ppm NH₃ and 500 ppm NO₂ in He flow followed by purging with He for 30 min, respectively. To ensure the reliability of DRIFT results, their relative amounts were also estimated from the NO oxidation activities of Cu-SSZ-13 and Cu-LTA (Supplementary Fig. S5) and the TPH measurements on the corresponding catalysts after fast SCR (NO₂/NO_x = 0.5) at 443 K for 60 min (Supplementary Fig. S7), respectively. It can be seen from Fig. 7 that the relative amount of NO₃⁻ is always larger in Cu-SSZ-13 than in Cu-LTA, regardless of the Cu/Al ratio. Also, its amount in both catalyst systems was found to generally increase with increasing Cu/Al ratio. Similar trends can be observed for the relative amounts of NH₄NO₃ in Cu-SSZ-13 and Cu-LTA. This is expected because NO₃⁻ anions are necessary to form NH₄NO₃ over copper-exchanged zeolite catalysts [46,47]. If such is the case, it would then be concluded that NH₄NO₃ formation, like NO₃⁻ one, is less feasible in Cu-LTA than in Cu-SSZ-13, because the main Cu²⁺ site in the former catalyst is the *s6rs* that are spatially more confined than 8-ring windows.

3.4. Catalytic comparison

Fig. 8 shows the NO_x conversion as a function of temperature in the

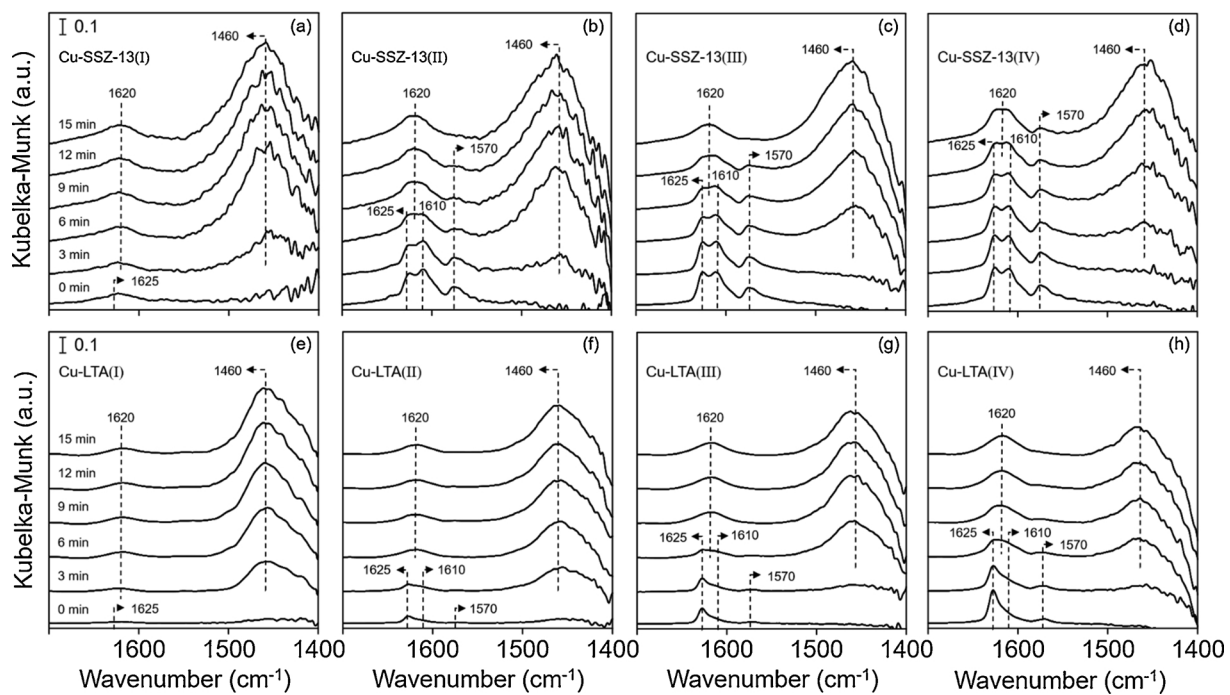


Fig. 5. Difference DRIFT spectra in the 1700–1400 cm^{−1} region of (a) Cu-SSZ-13(I), (b) Cu-SSZ-13(II), (c) Cu-SSZ-13(III), (d) Cu-SSZ-13(IV), (e) Cu-LTA(I), (f) Cu-LTA(II), (g) Cu-LTA(III), and (h) Cu-LTA(IV) recorded at 423 K during exposure to 500 ppm NH₃ in He flow for (from bottom to top) 0, 3, 6, 9, 12, and 15 min, respectively. In each panel, the bottom trace (i.e., the spectrum recorded in the absence of NH₃) was measured after exposure to 500 ppm NO and 5% O₂ in He flow at 423 K for 30 min followed by purging with He for 30 min (Supplementary Fig. S4).

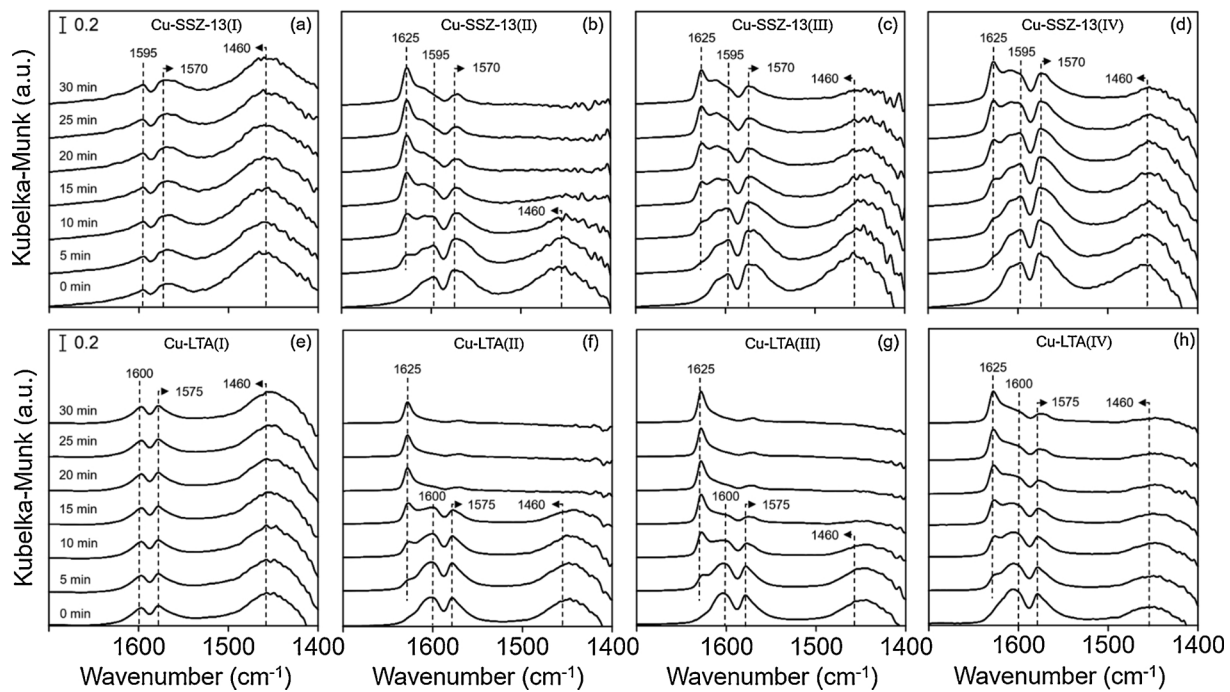


Fig. 6. Difference DRIFT spectra in the 1700–1400 cm^{−1} region of (a) Cu-SSZ-13(I), (b) Cu-SSZ-13(II), (c) Cu-SSZ-13(III), (d) Cu-SSZ-13(IV), (e) Cu-LTA(I), (f) Cu-LTA(II), (g) Cu-LTA(III), and (h) Cu-LTA(IV) obtained at 423 K during exposure to 500 ppm NO in He flow for (from bottom to top) 0, 5, 10, 15, 20, 25, and 30 min, respectively. In each panel, the bottom trace (i.e., the spectrum recorded in the absence of NO) was measured after exposure to 500 ppm NO₂ in He flow at 423 K for 30 min followed by purging with He for 30 min (Supplementary Fig. S6).

standard and fast SCR reactions over the series of Cu-SSZ-13 and Cu-LTA catalysts studied here. It is well established that fast SCR shows a higher deNO_x activity than the standard SCR, especially at temperatures lower than 523 K [5,40]. As expected, the low-temperature (< 523 K) activities over both catalysts are higher at NO₂/NO_x = 0.5 than at NO₂/NO_x = 0, whereas the opposite holds for their high-temperature

(> 673 K) activities. However, the extent of enhancement in the low-temperature activity is much larger over Cu-LTA than over Cu-SSZ-13, leading to a better deNO_x activity of the former catalyst in this low-temperature range, in contrast to the result obtained under the standard SCR conditions. Fig. 8 also shows that activity differences among the four Cu-LTA catalysts with different Cu/Al ratios at temperatures higher

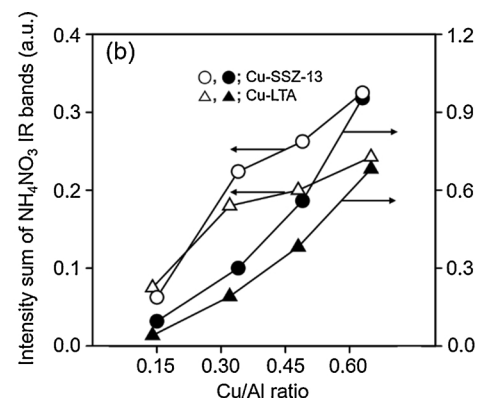
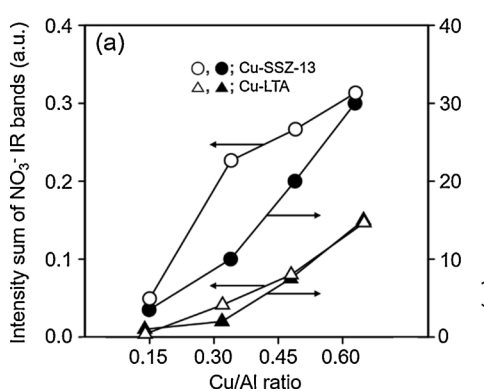


Fig. 7. (a) Intensity sum of the NO_3^- IR bands around 1625, 1610, and/or 1570 cm^{-1} (the bottom trace of each panel in Fig. 5) and NO oxidation conversion at 713 K (Supplementary Fig. S5) of each catalyst studied in this work vs its Cu/Al ratio and (b) Intensity sum of the NH_4NO_3 IR bands around 1600 and 1575 cm^{-1} (the bottom trace of each panel in Fig. 6) and area of the TPH peak from each zeolite-supported Cu catalyst after fast SCR ($\text{NO}_3/\text{NO}_x = 0.5$) at 443 K for 60 min (Supplementary Fig. S7) vs its Cu/Al ratio. The circle and triangle indicate Cu-SSZ-13 and Cu-LTA catalysts, respectively.

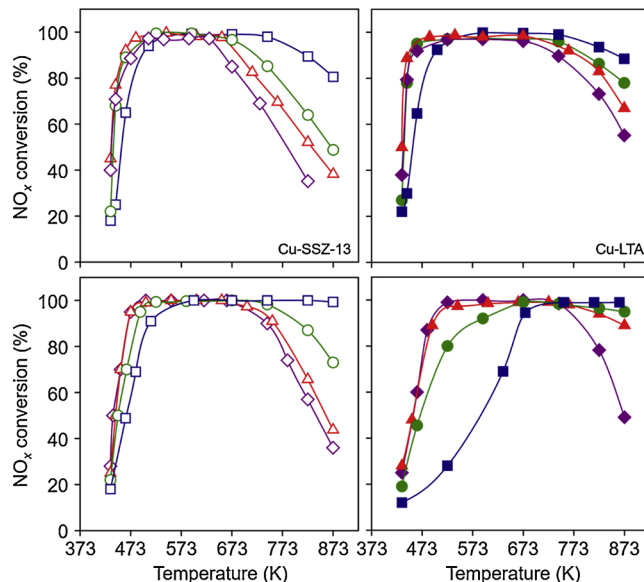


Fig. 8. NO_x conversion as a function of temperature in the standard (bottom) and fast (top) SCR reactions over Cu-SSZ-13(I) (□), Cu-SSZ-13(II) (○), Cu-SSZ-13(III) (△), Cu-SSZ-13(IV) (◇), Cu-LTA(I) (■), Cu-LTA(II) (●), Cu-LTA(III) (▲), and Cu-LTA(IV) (◆) catalysts. While the standard feed contains 500 ppm NH_3 , 500 ppm NO, 5% O_2 , 10% H_2O balanced with N_2 at $100,000\text{ h}^{-1}$ GHSV, fast SCR includes the injection of 250 ppm NO and 250 ppm NO_2 , instead of 500 ppm NO.

than 673 K under both standard and fast SCR conditions are smaller than those observed for the corresponding series of Cu-SSZ-13 catalysts, which could be primarily attributed to the lower NH_3 oxidation activities of the former catalysts [18].

NH_4NO_3 is also a key intermediate in fast SCR. Thus, the reaction between NH_4NO_3 and NO is the rate governing step to the low-temperature activity of this SCR [48,49]. If the formation of NH_4NO_3 is faster than its reduction, the “fast SCR” phenomenon would not be observed because of the inhibition effects of NH_4NO_3 on the SCR catalyst [9]. In this regard, the excellent low-temperature activity of Cu-LTA under the fast SCR conditions can be explained by considering that both formation and reduction of NH_4NO_3 is more efficient in Cu-LTA than in Cu-SSZ-13, as evidenced by the NO and NO_2 DRIFT results in Figs. 6 and 7 and Supplementary Fig. S6. Further, all Cu-LTA catalysts were found to produce a smaller amount of N_2O compared to the Cu-SSZ-13 catalysts (Supplementary Fig. S8). It thus appears that the NH_4NO_3 generated in the former catalyst system is mostly reduced by NO, rather than being thermally decomposed to N_2O .

To investigate the effects of NO_2 on the catalytic behavior of Cu-SSZ-13 and Cu-LTA catalysts, we measured the NO_x conversion as a function of NO_2/NO_x ratio at different temperatures (443–593 K). Here

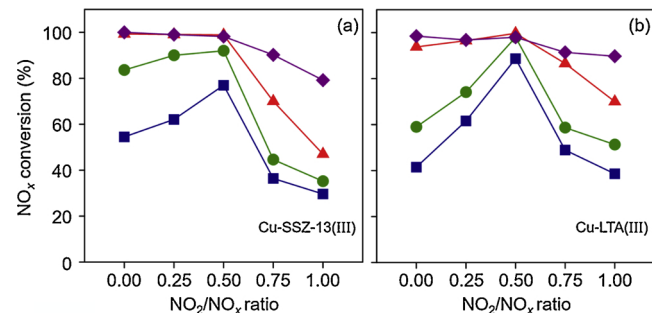


Fig. 9. NO_x conversion as a function of NO_2/NO_x ratio over (a) Cu-SSZ-13(III) and (b) Cu-LTA-16(III) with almost 100% copper exchange level at 443 (■), 463 (●), 523 (▲), and 593 (◆) K. The feed contains 500 ppm NH_3 , 500 ppm NO_x , 5% O_2 , 10% H_2O balanced with N_2 at $100,000\text{ h}^{-1}$ GHSV.

we selected Cu-SSZ-13(III) and Cu-LTA(III) as a representative catalyst of these two catalyst systems due to their remarkable low-temperature de NO_x activities (Fig. 8). It can be seen from Fig. 9 that the NO_x conversion is sensitive to the addition of NO_2 at 463 K or lower, while the highest catalytic activity for both catalysts is observed at a NO_2/NO_x ratio of 0.5, corresponding to equimolar amounts of NO and NO_2 . This indicates that the fast SCR conditions (i.e., $\text{NO}_2/\text{NO}_x = 0.5$) are most efficient for achieving the maximum NO_x conversion, as previously reported [40]. More interestingly, the activity enhancement by increasing NO_2/NO_x ratio up to 0.5 is higher over Cu-LTA(III) than over Cu-SSZ-13(III). This demonstrates that the former catalyst has a greater advantage in fast SCR than the latter one. Fig. 9 also shows that the extent of activity decrease at NO_2/NO_x ratios higher than 0.5 is lower over Cu-LTA(III) than over Cu-SSZ-13(III). As a result, the NO_x conversion of the former catalyst is higher than that of the latter one even under the slow SCR conditions ($\text{NO}_2/\text{NO}_x = 1$) in the temperature region tested. Considering that the excess NO_2 in the feed reacts with NH_3 and thus results in the formation of a significant amount of NH_4NO_3 responsible for catalyst deactivation, therefore, it can be concluded that NH_4NO_3 formation is less feasible over Cu-LTA than over Cu-SSZ-13.

4. Conclusions

We have carried out DRIFT measurements of adsorbed NO and NH_3 , temperature-programmed reduction of H_2 , SCR kinetics, and *in situ* DRIFT measurements using NH_3 , NO, and NO_2 molecules on four Cu-SSZ-13 and four Cu-LTA catalysts with the same bulk Si/Al ratio (16) but different Cu/Al ratios (0.14–0.65) in order to understand the characteristics of active sites in the latter catalyst system for the NH_3 -SCR reaction. It was found that while both Cu^{2+} and $[\text{Cu}(\text{OH})]^+$ ions exist in Cu-LTA, as well as in Cu-SSZ-13, their location in the former catalyst is substantially centered on the single 6-rings, especially when the Cu/Al ratio is 0.50 or lower. Unlike the case in Cu-SSZ-13 where the $[\text{Cu}]$

(OH)]⁺ ions occupy the 8-ring window sites even at a low Cu/Al ratio of < 0.2, the copper ions become located, mainly as [Cu(OH)]⁺, within the 8-ring windows in Cu-LTA when the Cu/Al ratio is higher than 0.5. We were also able to ascertain the formation of nitrate and ammonium nitrate reaction intermediates in both catalyst systems. However, relatively smaller amounts of these intermediates were formed in Cu-LTA compared to Cu-SSZ-13, regardless of the Cu/Al ratio, which can be attributed to the preferential location of copper ions near the single 6-rings in the former catalyst where the reactant molecules should be less accessible than the 8-ring window sites. As a result, Cu-LTA exhibits a higher activity under the fast SCR conditions than Cu-SSZ-13, in contrast to the trend observed under the standard SCR conditions.

Acknowledgements

This work was supported by the National Creative Research Initiative Program (2012R1A3A2048833) through the National Research Foundation of Korea and by the Korea Institute of Energy Technology Evaluation and Planning (20182020109770) and the Ministry of Trade, Industry & Energy of the Republic of Korea. We thank PAL for XANES beam time and K.-S. Lee (8C, PAL) for help in collecting XANES data. PAL is supported by MSIP and POSTECH.

Appendix A. Supplementary data

Supplementary material related to this article can be found, in the online version, at doi:<https://doi.org/10.1016/j.apcatb.2019.01.006>.

References

- [1] T.V. Johnson, Int. J. Engine Res. 10 (2009) 275–285.
- [2] M.V. Twigg, Catal. Today 163 (2011) 33–41.
- [3] R.O'Driscoll, H.M. ApSimon, T. Oxley, N. Molden, M.E.J. Stettler, A. Thiagarajah, Atmos. Environ. 145 (2016) 81–91.
- [4] U. Deka, I. Lezcano-Gonzalez, B.M. Weckhuysen, A.M. Beale, ACS Catal. 3 (2013) 413–427.
- [5] A.M. Beale, F. Gao, I. Lezcano-Gonzalez, C.H.F. Peden, J. Szanyi, Chem. Soc. Rev. 44 (2015) 7371–7405.
- [6] J. Wang, H. Zhao, G. Haller, Y. Li, Appl. Catal. B 202 (2017) 346–354.
- [7] M. Koebel, M. Elsener, G. Madia, Ind. Eng. Chem. Res. 40 (2001) 52–59.
- [8] C. Ciardelli, I. Nova, E. Tronconi, B. Bandl-Konrad, D. Chatterjee, M. Weibel, B. Krutzsch, Appl. Catal. B 70 (2007) 80–90.
- [9] J. Luo, Y. Tang, S. Joshi, K. Kamasamudram, N. Currier, A. Yezerets, SAE Tech. Pap. 10 (2017) 1691-01-0953.
- [10] S. Joshi, A. Kumar, J. Luo, K. Kamasamudram, N. Currier, A. Yezerets, Appl. Catal. B 226 (2018) 565–574.
- [11] M. Dusselier, M.E. Davis, Chem. Rev. 118 (2018) 5265–5329.
- [12] F. Gao, J. Szanyi, Appl. Catal. A 560 (2018) 185–194.
- [13] M. Moliner, C. Franch, E. Palomares, M. Grill, A. Corma, Chem. Commun. 48 (2012) 8264–8266.
- [14] N. Martín, C. Paris, P.N.R. Vennestrøm, J.R. Thøgersen, M. Moliner, A. Corma, Appl. Catal. B 217 (2017) 125–136.
- [15] J.H. Lee, Y.J. Kim, T. Ryu, P.S. Kim, C.H. Kim, S.B. Hong, Appl. Catal. B 200 (2017) 428–438.
- [16] D. Jo, T. Ryu, G.T. Park, P.S. Kim, C.H. Kim, I.-S. Nam, S.B. Hong, ACS Catal. 6 (2016) 2443–2447.
- [17] D. Jo, G.T. Park, T. Ryu, S.B. Hong, Appl. Catal. B 243 (2019) 212–219.
- [18] T. Ryu, N.H. Ahn, S. Seo, J. Cho, H. Kim, D. Jo, G.T. Park, P.S. Kim, C.H. Kim, E.L. Bruce, P.A. Wright, I.-S. Nam, S.B. Hong, Angew. Chem. Int. Ed. 56 (2017) 3256–3260.
- [19] N.H. Ahn, T. Ryu, Y.J. Kang, H. Kim, J. Shin, I.-S. Nam, S.B. Hong, ACS Catal. 7 (2017) 6781–6785.
- [20] M. Itakura, I. Goto, A. Takahashi, T. Fujitani, Y. Ide, M. Sadakane, T. Sano, Micropor. Mesopor. Mater. 144 (2011) 91–96.
- [21] Y.J. Kim, J.K. Lee, K.M. Min, S.B. Hong, I.-S. Nam, B.K. Cho, J. Catal. 311 (2014) 447–457.
- [22] J.H. Kwak, T. Varga, C.H.F. Peden, F. Gao, J.C. Hanson, J. Szanyi, J. Catal. 314 (2014) 83–93.
- [23] F. Giordanino, P.N.R. Vennestrøm, L.F. Lundsgaard, F.N. Stappen, S.L. Mossin, P. Beato, S. Bordiga, C. Lamberti, Dalton Trans. 42 (2013) 12741–12761.
- [24] K. Xie, J. Woo, D. Bernin, A. Kumar, K. Kamasamudram, L. Olsson, Appl. Catal. B 241 (2019) 205.
- [25] C. Negri, P.S. Hammershøi, T.V.W. Janssens, P. Beato, G. Berlier, S. Bordiga, Chem. Eur. J. 24 (2018) 12044.
- [26] G.T. Palomino, S. Bordiga, A. Zecchina, G.L. Marra, C. Lamberti, J. Phys. Chem. B 104 (2000) 8641–8651.
- [27] J.H. Kwak, J.H. Lee, S.D. Burton, A.S. Lipton, C.H.F. Peden, J. Szanyi, Angew. Chem. Int. Ed. 52 (2013) 9985–9989.
- [28] R. Zhang, J.-S. McEwen, M. Kollár, F. Gao, Y. Wang, J. Szanyi, C.H.F. Peden, ACS Catal. 4 (2014) 4093–4105.
- [29] J. Sarkany, Phys. Chem. Chem. Phys. 1 (1999) 5251–5257.
- [30] J.H. Kwak, H. Zhu, J.H. Lee, C.H.F. Peden, J. Szanyi, Chem. Commun. 48 (2012) 4758–4760.
- [31] J. Luo, D. Wang, A. Kumar, J. Li, K. Kamasamudram, N. Currier, A. Yezerets, Catal. Today 267 (2016) 3–9.
- [32] J. Luo, F. Gao, K. Kamasamudram, N. Currier, C.H.F. Peden, A. Yezerets, J. Catal. 348 (2017) 291–299.
- [33] R. Bulánek, B. Wichterlová, Z. Sobalík, J. Tichý, Appl. Catal. B 31 (2001) 13–25.
- [34] F. Gao, E.D. Walter, E.M. Karp, J. Luo, R.G. Tonkyn, J.H. Kwak, J. Szanyi, C.H.F. Peden, J. Catal. 300 (2013) 20–29.
- [35] F. Gao, D. Mei, Y. Wang, J. Szanyi, C.H.F. Peden, J. Am. Chem. Soc. 139 (2017) 4935–4942.
- [36] S.A. Bates, A.A. Verma, C. Paolucci, A.A. Parekh, T. Ang-gara, A. Yezerets, J. Catal. 312 (2014) 87–97.
- [37] F. Gao, E.D. Walter, N.M. Washton, J. Szanyi, C.H.F. Peden, ACS Catal. 3 (2013) 2083–2093.
- [38] J. Song, Y.L. Wang, E.D. Walter, N.M. Washton, D.H. Mei, L. Kovarik, M.H. Engelhard, S. Prodinger, Y. Wang, C.H.F. Peden, F. Gao, ACS Catal. 7 (2017) 8214–8227.
- [39] K. Hadjiiivanov, Catal. Lett. 68 (2000) 157–161.
- [40] I. Nova, E. Tronconi (Eds.), Urea-SCR Technology for deNOx After Treatment of Diesel Exhausts, Springer, 2014.
- [41] M.P. Ruggeri, I. Nova, E. Tronconi, J.A. Pihl, T.J. Toops, W.P. Partridge, Appl. Catal. B 166 (2015) 181–192.
- [42] T.V.W. Janssens, H. Falsig, L.F. Lundsgaard, P.N.R. Vennestrøm, S.B. Rasmussen, P.G. Moses, F. Giordanino, E. Borfecchia, K.A. Lomachenko, C. Lamberti, S. Bordiga, A. Godiksen, S. Mossin, P.A. Beato, ACS Catal. 5 (2015) 2832–2845.
- [43] A. Godiksen, P.N.R. Vennestrøm, S.B. Rasmussen, S. Mossin, Top. Catal. 60 (2017) 13–29.
- [44] S. Elzey, A. Mubayi, S.C. Larsen, V.H. Grassian, J. Mol. Catal. A 285 (2008) 48–57.
- [45] D. Wang, L. Zhang, K. Kamasamudram, W.S. Epling, ACS Catal. 3 (2013) 871–881.
- [46] G. Delahay, B. Coq, S. Kieger, B. Neveu, Catal. Today 54 (1999) 431–438.
- [47] H. Chen, Z. Wei, M. Kollar, F. Gao, Y. Wang, J. Szanyi, C.H.F. Peden, J. Catal. 329 (2015) 490–498.
- [48] C. Ciardelli, I. Nova, E. Tronconi, D. Chatterjee, B. Bandl-Konrad, Chem. Commun. 23 (2004) 2718–2719.
- [49] M. Bendrich, A. Scheuer, R.E. Hayes, M. Votsmeier, Appl. Catal. B 222 (2018) 76–87.